Vol 14 No 12, December 2005
1009-1963/2005/14(12)/2560-05

Chinese Physics

© 2005 Chin. Phys. Soc.
and IOP Publishing Ltd

A numerical simulation of the backward Raman amplifying in plasma*

Wang Hong-Yu(王虹宇)[a)b)] and Huang Zu-Qia(黄祖洽)[a)]

[a)] *Institute of Low Energy Nuclear Physics, Beijing Normal University, Beijing* 100875, *China*

[b)] *Department of Physics, Anshan Normal University, Anshan* 114005, *China*

(Received 12 October 2005)

This paper describe a numerical simulation method for the interaction between laser pulses and low density plasmas based on hydrodynamic approximation. We investigate Backward Raman Amplifying (BRA) experiments and their variants. The numerical results are in good agreement with experiments.

Keywords: plasma simulation, laser plasma interactions, backward Raman amplifier
PACC: 5265, 4265K, 5240D

1. Introduction

Recently, the concept of laser amplifying by backward Raman scattering (backward Raman amplifiers, BRA) in plasma was presented,[1−4] in which a short seed pulse is amplified by a counter-propagating long pumping pulse when the resonance relation $\omega_{\rm seed} + \omega_{\rm plasma} = \omega_{\rm pump}$ is satisfied. In the nonlinear regime, the seed pulse is strongly amplified and compressed temporally. Theoretically, unfocused intensities of $10^{17}{\rm W/cm}^2$ in 50fs pulses are accessible by this technique.

Up to now two schemes of BRA have been presented: the amplifier in the non-linear regime and in the transient regime. The basic concepts of the first scheme are based on the π-pulse solutions of laser–plasma coupled equations.[2] When the amplitudes of the plasma wave and the seed pulse are both quite large, the pumping pulse's energy is absorbed by the front of the seed pulse. So the front edge of the seed pulse is amplified while the back edge will be reduced for the energy feedback into the exhausted pumping pulse. In this way, the seed pulse is amplified and compressed. Finally, the seed pulse evolves to a narrow wave train which is called a π pulse.

The scheme of transient BRA is based on the matching of the plasma's density gradient and the pumping pulse's frequency chirp.[4,5] In the amplifying process, a strict matching of the two pulses and the plasma frequency is always needed. If we let the pumping pulse chirp and the plasma density have a gradient, and set the plasma frequency gradient to just be a half of the pumping chirp gradient, the seed pulse will be amplified only at a fixed position of itself. By passing a plasma of sufficient length, the amplifying takes place and an ultra-fast laser pulse formed.

Each scheme is very difficult to be realized. For the limit of plasma technology, the density of gas-jet plasma is limited to about $10^{19}{\rm cm}^{-3}$ at present. To get distinct amplification, the seed pulse must travel several millimetres in plasma. The amplification requires a rigorous match of the frequencies. Keeping the uniformity of the plasma is a great challenge in experiments. In the transient scheme, we need even longer plasma length to compensate for the lower efficiency.

However, some good results of amplifying experiments have been posted recently.[6,7] Especially, experiments have shown that the non-linear BRA scheme was possible. In the experiments by Cheng *et al*,[7] the seed pulses were amplified to one order higher than the pumping pulse and the amplifying ratio was several thousands.

Consequently, the numerical simulation of BRA becomes a valuable problem in computational plasma physics. However, compared with the common plasma simulations there are some special difficulties because of the long-distance travelling wave.[8−10] First, the

*Project supported by Ph.d Foundation of China Education (Grant No 20020027006).

computing time and memory needed is very large. Second, the investigation requires low-error simulation technology for the low increase rates of Raman effects. For example, we need a great number of particles to get rid of the numerical wave-breaking and numerical heating in the particle-in-cell method.[11] Besides, we need a high-order difference scheme of the electromagnetic field equation to overcome the difficulties of numerical dispersion while applying it to the long-distance travelling wave. So the simulations of BRA are mainly focused on two regimes now: (1) averaging the effects of electromagnetic fields to reduce the spacetime steps, such as the APIC method,[12] and (2) using the amplitudes coupled equations[13−15] or linearized plasma wave equations to get approximate analysis.

An attractive idea is applying a moving window following the seed pulse to the computation. This technology is convenient to investigate the interactions between laser and low-density plasma. In the corona region, the plasma density is about $\frac{1}{10}$ to $\frac{1}{100}$. The group velocity of laser pulse is very close to the light speed. So the calculated window is shorter than $\frac{1}{10}$ of the total interaction region. There is a simulation method which applies a moving window on the standard PIC simulation (moving window PIC simulation, MWPIC).[16] However, MWPIC needs the spacetime step match ($\mathrm{d}x = c\mathrm{d}t$) to avoid interpolation error. The step setting is unstable at two-dimensional and three-dimensional explicit differential schemes. That means we need some implicit differential schemes. The latter technology is still developing. In addition, MWPIC needs a very large number of particles to get acceptable precision.

For the above reasons, we developed a numerical simulation technique based on hydrodynamic approximation. In this technique, we only use the cold-plasma approximation which is often used in theoretical researches. The numerical trials indicate that the technique is suitable for the travelling wave problems in plasmas and can give results in concordance with experiments. Besides, the technique has a clear physical picture and the results can be easily analysed.

We will discuss the BRA equations and the simulation technology in Sections 2 and 3, then analyse the numerical results in Section 4.

2. The basic equation of BRA

In the typical instance of BRA, we can introduce the cold-plasma approximation and the transverse canonical momentum conservation:[17] $\boldsymbol{v} = \boldsymbol{u} + \frac{e\boldsymbol{A}}{\gamma mc} = \boldsymbol{u} + c\boldsymbol{a}$, where $\boldsymbol{u}$ is the longitude velocity and $\boldsymbol{A}$ is the vector potential at Coulomb gauge while $\boldsymbol{a}$ is the normalized vector potential: $\boldsymbol{a} = \frac{e\boldsymbol{A}}{mc^2}$. Because the electrons' velocities are far less than the light speed, we can ignore the relativistic factor γ.

The plasma hydrodynamic equation can be written as (we ignore the thermal pressure here; we can recover it in the rhs of the second equation whenever needed)

$$\frac{\partial n}{\partial t} + \nabla(n\boldsymbol{v}) = 0, \tag{1}$$

$$\frac{\partial \boldsymbol{v}}{\partial t} + (\boldsymbol{v}\cdot\nabla)\boldsymbol{v} = -\frac{e\boldsymbol{E}}{m} - \frac{e(\boldsymbol{v}\times B)}{mc}. \tag{2}$$

Supposing the plasma flow is non-vertex before the laser action and applying the cold-plasma approximation, we get the plasma hydrodynamic equation:

$$\frac{\partial n}{\partial(ct)} + (\boldsymbol{\beta}\cdot\nabla)n = -n(\nabla\cdot\boldsymbol{\beta}) - (\boldsymbol{a}\cdot\nabla)n, \tag{3}$$

$$\frac{\partial \gamma\beta}{\partial(ct)} + (\boldsymbol{\beta}\cdot\nabla)\boldsymbol{\beta} = \nabla\phi - \frac{1}{2}\nabla\boldsymbol{a}^2 - \nabla(\boldsymbol{\beta}\cdot\boldsymbol{a}). \tag{4}$$

The electromagnetic field satisfies the wave equation and Poisson equation:

$$\left(\frac{1}{c^2}\frac{\partial^2}{\partial t^2} - \nabla^2\right)\boldsymbol{a} = -\frac{4\pi ne^2}{mc^2}\boldsymbol{a}, \tag{5}$$

$$\nabla^2\phi = \frac{4\pi e^2}{mc^2}(n - n_i). \tag{6}$$

Applying the coordinate transformation

$$\xi = x - ct, \tag{7}$$

$$\eta = t, \tag{8}$$

we get the wave equation in the new variables:

$$\left(\frac{1}{c^2}\frac{\partial^2}{\partial\eta^2} - \frac{2}{c}\frac{\partial^2}{\partial\xi\partial\eta} - \frac{\partial^2}{\partial y^2} - \frac{\partial^2}{\partial z^2}\right)\boldsymbol{a} = -\frac{4\pi ne^2}{mc^2}\boldsymbol{a}, \tag{9}$$

and the Poisson equation has no change.

To solve the wave equation numerically, we introduce the medium variable $\boldsymbol{\psi}$:

$$\left(\frac{1}{c}\frac{\partial}{\partial\eta} - 2\frac{\partial}{\partial\xi}\right)\boldsymbol{a} = \boldsymbol{\psi}.$$

Finally, we get a pair of first order differential equations:

$$\begin{aligned}\frac{\partial\boldsymbol{\psi}}{\partial\eta} &= -\frac{4\pi ne^2}{mc^2}\boldsymbol{a} + \nabla_\perp^2\boldsymbol{a},\\ \frac{1}{c}\frac{\partial\boldsymbol{a}}{\partial\eta} &= \boldsymbol{\psi} + 2\frac{\partial a}{\partial\xi}.\end{aligned} \tag{10}$$

With the same transformation, the hydrodynamic equations become

$$\begin{aligned}
&\frac{\partial n}{\partial t}+(\beta_x-1)\frac{\partial n}{\partial x}+\beta_y\frac{\partial n}{\partial y}\\
=&-n\left[\frac{\partial(\beta_x-1)}{\partial x}+\frac{\partial\beta_y}{\partial y}\right],\\
&\frac{\partial\beta_x}{\partial t}+\left[(\beta_x-1)\frac{\partial}{\partial x}+u_y\frac{\partial}{\partial y}\right](\beta_x-1)\\
=&\frac{\partial\phi}{\partial x}-\frac{1}{2}\frac{\partial \boldsymbol{a}^2}{\partial x},\\
&\frac{\partial\beta_y}{\partial t}-\left[\frac{\partial}{\partial x}+\beta_y\frac{\partial}{\partial y}\right]\beta_y\\
=&\frac{\partial\phi}{\partial y}-\frac{1}{2}\frac{\partial \boldsymbol{a}^2}{\partial y}.
\end{aligned}\tag{11}$$

The equations (6), (10, (11) are the basic equations to describe the laser–plasma interactions in BRA.

3. Numerical simulation method

The electromagnetic equations (6), (10) describe the electromagnetic wave transmitting in plasma. In BRA scheme, the transverse dynamic effects are mainly slow processes such as self-focusing. We can use the periodic boundary conditions in the transverse directions, apply FFT calculation to eliminate the transverse derivatives and use direct elimination technology in the longitudinal direction. So we will focus on the one-dimensional scheme at following discussion. However, the generalization to multi-dimensions is straightforward.

The elimination of Poisson equation is quite simple. In our moving window, the right boundary of calculating region are always at the front of seed pulse. We ignore the interactions between the pumping pulse and the origin plasmas for the uniform of the pumping pulse, so all laser-plasma interaction can not affect the region in the right side of the boundary. Then we can assume that there are no electrostatic fields in the right region of seed pulse: $\boldsymbol{E}=0$ then $\phi_i=\phi_{i+1}=\cdots=\text{const}$. The differential scheme is

$$\phi_{i-1}=\frac{4\pi e^2}{mc^2}\delta x^2(n_i-N_i)-\phi_{i+1}+2\phi_i. \tag{12}$$

To get the numerical solution of the wave equation,we use a generation of Liu's leapfrog-upwind scheme:[18]

$$\begin{aligned}
&\frac{\frac{1}{2}[(a_{i-1}^{n+1}-a_{i-1}^{n})+(a_i^n-a_i^{n-1})]}{\delta t}\\
&-2c\frac{\frac{1-m}{2}(a_{i+1}^n-a_i^n)+m(a_i^n-a_{i-1}^n)+\frac{1-m}{2}(a_{i-1}^n-a_{i-2}^n)}{\delta x}\\
=&\frac{1}{2}c(\psi_i^n+\psi_{i-1}^n),
\end{aligned}\tag{13}$$

where

$$\kappa=2c\frac{\delta t}{\delta x}, \tag{14}$$

$$m=\frac{1}{6}(5+3\kappa-2\kappa^2), \tag{15}$$

$$\begin{aligned}
a_i^{n+1}=&a_{i+1}^{n-1}-(1-2m\kappa)(a_{i+1}^n-a_i^n)\\
&+(1-m)\kappa(a_{i+2}^n-a_{i+1}^n)\\
&+(1-m)\kappa(a_i^n-a_{i-1}^n)\\
&+c\delta t(\psi_{i+1}^n+\psi_i^n).
\end{aligned}\tag{16}$$

The hydrodynamic equation (11) can be solved with the leap-frog method too. However, we must apply the FCT technology[19] to avoid the numerical oscillation while introduce little numerical damping. The Flux Corrects are used in all leap-frog steps by rewriting the convection equations:

$$\frac{\partial U}{\partial t}+\frac{\partial F}{\partial x}=S, \tag{17}$$

where F means the convect terms and S means source terms, and then the leap-frog scheme is

$$\begin{aligned}
U_i^{n+1}=&U_i^{n-1}-2\frac{\Delta t}{\Delta x}(F_{i+1/2}^n-F_{i-1/2}^n)\\
&+2\Delta t S_i^n.
\end{aligned}\tag{18}$$

To use FCT technology, first we calculate the low-order flux of plasma density (there is no source term in the continuum equation):

$$F_{i+1/2}^{\text{low}}=\overline{v_i}\times n_i^{\text{DC}}\times\delta t+\eta(n_{i+1}^{k-1}-n_i^{k-1}), \tag{19}$$

$$\overline{v_i}=\frac{1}{2}(v_i^k+v_{i+1}^k), \tag{20}$$

$$\text{if} \quad (\overline{v} \geq 0) w_i^{\mathrm{DC}} = w_i^{k-1}, \tag{21}$$

$$\text{else} \quad w_i^{\mathrm{DC}} = w_{i+1}^{k-1}, \tag{22}$$

$$w = n, v, \tag{23}$$

η is a coefficient about $\frac{1}{24}$ to $\frac{1}{8}$. The smaller η means less error but more numerical oscillation. Then the high-order flux is

$$F_{i+\frac{1}{2}}^{\mathrm{high}} = \frac{7}{12}(f_{i+1} + f_i) - \frac{1}{12}(f_{i+2} + f_{i-1}). \tag{24}$$

We do not introduce the correction of the velocity's flux because it will cause much damping in the simulation. So the velocity flux can use the same scheme as the high-order density flux.

However, the difference scheme of plasma density does not preserve positivity. To get rid of the difficulties of negative electron density, we apply a limiter of density flux: the out-flux density cannot exceed the present electron density of each point. The physics of this limiter are clear.

4. Numerical results and the analysis

Cheng's experiment results[7] were the best experiment validation of the BRA scheme. In this experiment, the author amplified the seed pulse in a gas-jet plasma. In the plasma with 2mm effective length, the intensities of seed pulses were amplified several thousands times and the length of seed pulses was compressed from 550fs (origin) to about 150fs. The recorded intensity reached $1.7 \times 10^{15}\mathrm{W/cm^2}$ which was higher than pump intensity by more than 1 order in magnitude. The author recorded the broadened (800fs) and compressed ($<$ 200fs) output pulses both in the experiment, which informed that the amplifying process had been in non-linear region.

We investigated the process numerically. As the experiments setting up, we set the seed pulse length to 550 fs and set the pumping pulse length to 10ps. The plasma's length was about 2mm and the plasma's density was $1.1 \times 10^{19}\mathrm{cm^{-3}}$. The wavelength of pumping pulse was 0.8μm and the wavelength of seed pulse was set to matching with the plasma and pumping pulse.

At the peak top of the pumping pulse,we let the two pulses collide each other. For the uncertainty of the collide points and the plasma temperatures, the simulating results varied a little. When the interaction finished, the seed pulse evolved to narrow peek which FWHM about 150–170fs and peak intensity about $1.5 \times 10^{15} - 1.9 \times 10^{15}\mathrm{W/cm^2}$. The typical simulate results were shown at Fig.1. We can find that the π-pulse shape easily. Which means the non-linear amplifying region was reached. Considered the uncertainly of the plasma temperature and length, we can find good agreement between the simulations and the experiments.

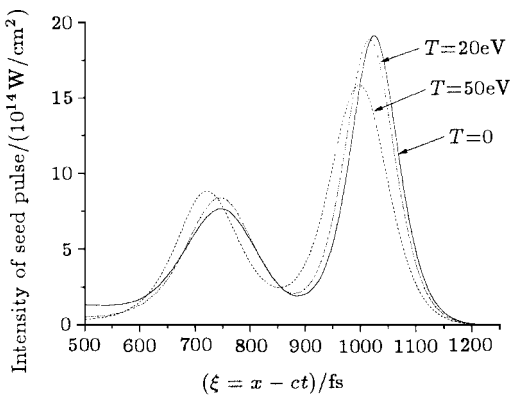


Fig.1. The output intensity versus ξ after amplified.

From the simulation results, we can find the evolving process of seed pulse. Let the seed pulse collide with different length pumping pulse; we can image the evolution of the seed pulse: it broadened to about 750 fs and compressed later. At the end, it evolved to a pulse shorter than 160 fs.

Typical results are shown at Fig.2.

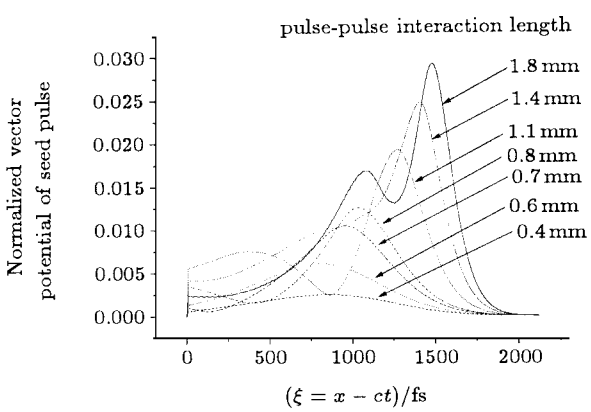


Fig.2. The amplified pulse shape of the seed by different length pumping pulse.

The simulating process shows the non-linear character of plasma wave. When the amplitude of plasma wave is quite large, the wave shape is different from sine wave; the typical wave form is shown in Fig.3. As we see, the difference is quite evident in our results. In fact, the effective $\delta n/n$ can exceed 1 when the amplifier reaches the exhaust region. This phenomenon made an added stability of amplifier from wave-breaking.

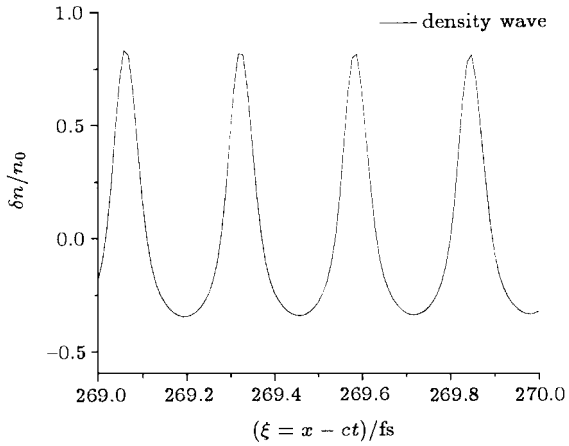


Fig.3. The typical wave-shape of density oscillating when the amplitudes become large.

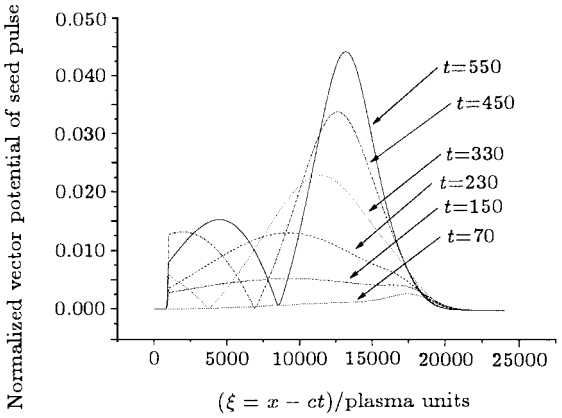


Fig.4. The pulse shape of the seed after being amplified by different length pumping pulse; the unit is the natural of plasma.

However, our results show that when the amplifying length reached 2mm, the plasma wave amplitude was close to the cold plasma wave-breaking amplitude, which means that, if we want to make a practical amplifier, we must increase the plasma density to get higher stabilities. Although it was very difficult to get dense and uniform plasma in experiments, we simulated the BRA process in a quite dense plasma ($n = 0.04n_{\rm cr}$). The results were coarse in precision but show that the amplifying processes were much more stable and that it was easier to reach the nonlinear regime in a denser plasma. The higher increase rates of Raman effects and higher stability compensated for the lower conversion effects in the denser plasmas. The results of our simulation are shown in Fig.4. In this density, we need shorter than 1mm plasmas to generate obviously amplified intensities. This means that the increasing of uniform plasma density should be the most important improvement at future experiments.

Our method can be easily improved to include the effects as pumping heat, plasma un-uniformity, inverse-Bremsstrahlung, or even linear Landau damping, tunnel-ionized (by phenomena) effects, etc. The investigation of these effects in BRA are proceeding now.

5. Conclusion

We introduced a hydrodynamic simulation method which was suitable for the interaction of lasers and corona plasmas. The method is convenient for the simulation of ultra-fast laser's transmitting. We simulated the Backward Raman Amplifiers experiments numerically, and the results show good agreement with experiments. The following study will appear in another paper.

Acknowledgment

Professor Chen Bao-Zhen has given some constructive suggestions about this work.

References

[1] Shvets G, Fisch N J, Pukhov A and Meyertervehn J 1998 *Phys. Rev. Lett.* **81** 4879
[2] Malkin V M, Shvets G and Fisch N J 1999 *Phys. Rev. Lett.* **82** 4448
[3] Clark D S and Fisch N J 2002 *Phys. Plasmas* **9** 2272
[4] Malkin V M, Shvets G and Fisch N J 2000 *Phys. Plasmas* **7** 2232
[5] Malkin V M, Shvets G and Fisch N J 2000 *Phys. Rev. Lett.* **84** 1209
[6] Ping Y, Cheng W *et al* 2004 *Phys. Rev. Lett.* **92** 175007
[7] Cheng W, Avitzour Y *et al* 2005, *Phys. Rev. Lett.* **94** 045003
[8] Zhang Q J,Sheng Z M and Zhang J 2004 *Chin. Phys.* **13** 905
[9] Xu H, Chang W W and Zhuo H B 2003, *Chin. Phys.* **12** 135
[10] Clark D S and Fisch N J 2003 *Phys. Plasmas* **10** 4848
[11] Birdsall C K and Langdon A B 1991 *Plasma Physics via Computer Simulation* (London:IOPP)
[12] Hur M S *et al* 2004 *Phys. Plasmas* **11** 5204
[13] Fraiman G M, Yampolsky N A *et al* 2002 *Phys. Plasmas* **9** 3617
[14] Tsidulko Y A, Malkin V M and Fisch N J 2002, *Phys. Rev. Lett.* **88** 235004
[15] Berger R L, Clark D S, Solodov A A *et al* 2004 *Phys. Plasmas* **11** 1931
[16] Nieter C and Cary J R 2004 *J. Comput. Phys.* **196** 478
[17] Sprangle P, Esarey E, Ting A and Joyce G 1998 *Appl. Phys. Lett.* **53** 2146
[18] Liu R X and Shu Q W 2003 *Some New Methods of Computernal Fluid Mechanics* (Chinese Science Press) (in Chinese)
[19] Zalesak S T 1979 *J. Comput. Phys.* **31** 335